Flow dynamic of human cough and measuring techniques: A review

Chen Zhang*[1], Peter V. Nielsen[1], Simon Madsen[1], Li Liu[2], Chunwen Xu[3], Zhengtao Ai[4]

1 Department of the Built Environment
Aalborg University
Denmark
Corresponding author: cz@build.aau.dk

2 Department of Building Science
Tsinghua University
China

3 College of Pipeline and Civil Engineering
China University of Petroleum (East China)
China

4 Department of Building Environment and Energy
Hunan University
China

ABSTRACT

Coughing is one of the most important respiratory activities for air transmitted pathogens. It is essential to understand the dispersion of exhaled particles when coughing to improve the prevention measure and reduce the cross-infection risk. However, cough flow structure is complex and influenced by many parameters. Simplifications are often made to the initial flow condition when simulating the transport of particles expelled during coughing in laboratory or numerical studies . This study conducts a systematic literature review on human cough, especially focusing on flow dynamic characterization. First, the measuring techniques for identifying the airflow characteristic are summarized. The boundary conditions for cough, such as flow profile, flow direction, cough duration and are compared between different studies. Finally, the vortex structure of cough and its impact on cough particle dispersion is discussed.

KEYWORDS

COVID-19, cough, respiratory infectious disease, flow dynamic, particle deposition, flow profile

1   INTRODUCTION

The COVID-19 pandemic is a respiratory infectious disease, and it has caused global health concerns. WHO has reported that the virus can spread from an infected person's mouth or nose in small particles when they cough, sneeze, speak, sing or breathe (WHO 2021). Compared with other respiratory activities like breath or speak, cough generates a higher expiratory velocity and contains a higher aerosol concentration, which leads to a potentially higher risk of cross-infection. Centers for Disease Control and Prevention (CDC 2021) has pointed out that the '2 meters (6-feet) rule' might not apply to situations involving increased exhalation, e.g. coughing. It is essential to understand the dispersion of exhaled particles when coughing to improve the prevention measure and reduce the cross-infection risk.
A cough is a reflex action to clear the airways of mucus and irritants such as dust or smoke. It normally includes three phases: inspiratory, compressive, and expiratory phases. The inspiratory phase is associated with glottic opening and the inhalation of variable amounts of air. The compressive phase consists of closure of the glottis and contraction of the expiratory muscles resulting in raised intra- thoracic pressure. In the expiratory phase the glottis opens suddenly, causing an explosive release of the trapped intrathoracic air (Mahajan et al. 1994).

Cough flow structure is complex, and is influenced by many parameters such as the cougher's age, gender, and posture, which consequently affect particle dispersion indoors (Muthusamy et al. 2021). However, simplifications are often made to the initial flow condition in laboratory or numerical studies when simulating the transport of droplets expelled during coughing (Gupta, Lin, and Chen 2009a).

This study aims to conduct a systematic literature review on human cough, especially focusing on flow dynamic characterization. First, the measuring techniques for identifying the airflow characteristic of cough are summarized. The boundary conditions for cough, such as flow profile, flow direction, cough duration and are compared between different studies. Finally, the vortex structure of cough and its impact on cough particle dispersion is discussed.

2   FLOW DYNAMIC CHARACTERISTICS OF COUGH

2.1   Cough flow profile

Based on the literature (Mahajan et al. 1994)(Khan et al. 2004)(Gupta et al. 2009a)(Oh et al. 2022), the time-series cough profile can be illustrated in Figure 1. The profile indicates that the cough starts with a short inhalation, follows by a dramatic acceleration in exhalation and finally a slow decay. The inhalation volume is very small and can be neglected. The characteristic of the cough profile can be defined by the following parameters: peak flow rate (PFR) or peak velocity (PV); peak velocity time (PVT), and cough duration time (CDT) and cough expired volume (CEV) is the area under the curve. Besides the parameters mentioned above, flow direction and mouth opening are important to describe the flow characteristic of cough. Table 1 summarizes the measuring techniques and flows dynamic characteristics of cough from literature studies.
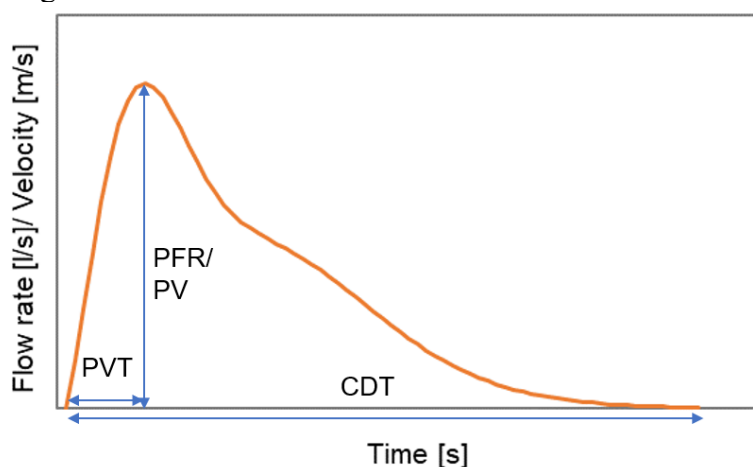

Figure 1. Cough profile as a function of time. Peak flow rate (PFR) or peak velocity (PV); peak velocity time (PVT), and cough duration time (CDT) and cough expired volume (CEV) is the area under the curve.

Depending on the measurement techniques, cough peak flow rate PFR was measured in the studies using spirometer (Lindsley et al. 2010)(Gupta, Lin, and Chen 2009b)(Mahajan et al. 1994), and peak velocity PV was measured using Schlieren imaging (Tang et al. 2012) or PIV (Han et al. 2021)(Khan et al. 2004)(Zhu, Kato, and Yang 2006)(Chao et al. 2009)(Vansciver, Miller, and Hertzberg 2011)(Kwon et al. 2012)(Wang et al. 2020). Some studies (Oh et al. 2022) attempt to convert these two parameters by considering the mouth opening area, however, assumptions have to be made by using the average mouth opening area without considering the individual difference and the mouth opening area keeps constant during the whole cough process.

Gupta et al. (2009b) measured cough flow rates from 25 subjects, and a large variation existed among the subjects, especially between males and females. For males, the PFR ranged from 3 to 8.5 l/s, while the value for females was 1.6 – 6 l/s. Lindsley et al. (2010) investigated the

influenza virus produced by coughing. The influenza-negative subjects produced slightly higher PFR than influenza-positive subjects, where the average values are 7.6 l/s and 7.1 l/s, respectively.

Table 1. Measurement techniques and flow dynamic characteristics of cough

Reference	Technique	Subjects	Cough Duration [s]	Cough peak velocity [m/s] or flow rate [l/s]	Peak velocity time [ms]	Cough Volume [l]	Flow direction	Mouth geometry
(Mahajan et al. 1994)	spirometer	10		2.8-15.8 l/s	10-50	0.5-5		
(Khan et al. 2004)	PIV	5 (4 M and 1 F)	0.9	8.1 m/s				
(Zhu 2006)	PIV	3 (3 M)	0.5	6-22 m/s Average: 11.2 m/s		0.8-2.2 Average 1.4		
(Gupta et al. 2009b)	Spirometer	25 (13 M and 12 F)	0.35-0.75	M:3-8.5 L/s F:1.6-6 L/s	M: 57-96 F: 57-110	M:0.4-1.6 F:0.25-1.25	$\theta1=15\pm5$ °; $\theta2=40\pm4$ ° (vertical spread angle 25 °)	Mouth opening area: M:400 ± 95 mm^2 F:337 ± 140 mm^2
(Chao et al. 2009)	PIV	11 (3 M and 8 F)		M:13.2 m/s F: 10.2 m/s Average 11.7 m/s				
(Lindsley et al. 2010)	Spirometer	58 (47 influenza-positive and 11 influenza-negative	0.9	Influenza-positive 7.1 l/s Influenza-negative 7.6 l/s		Influenza-positive 2.7 Influenza-negative 3.1		
(Vansciver et al. 2011)	PIV	29 (10 M and 19 F)	0.55	1.15-28.8 m/s Average 10.2m/s				706 (D= 30 mm)
(Tang et al. 2012)	schlieren imaging technique	20 (10 M and 10 F)	0.2-0.35	M:3.2–14 m/s F: 2.2–5.0 m/s;				
Kwon S. et al. (Kwon et al. 2012)	PIV	26 (17 M and 9 F)		M: 15.3 m/s F 10.6 m/s			Vertical spread angle M: 38 ° F: 32 °	
(Wang et al. 2020)	PIV	4		15 m/s				

(Han et al. 2021)	PIV	10 (5 M and 5 F)	0.52-0.56	M:6.4-18.6 m/s F: 5.0-15.7 m/s	M: 8-35 F: 8-39		Vertical spread angle M: 15.3 ° F: 15.6 ° Horizontal spread angle M: 13.3 ° F: 14.2 °	Mouth width M: 47 mm F: 39.4 mm

Note: M represents male, and F represents female.

A large variation also exists in the peak velocity PV. The largest variation was observed by Vansciver et al. (2011), where the PV ranged from 1.15 m/s to 28.8 m/s from the measurement of 29 healthy subjects. The gender difference on PV was pointed out by several studies (Chao et al. 2009)(Tang et al. 2012)(Kwon et al. 2012)(Han et al. 2021). In general, PV for females was weaker than that for males. Bianchi and Baiardi (2008) further correlated PV with the subjects' gender, height, age and body mass surface through regression analysis. The differences on cough PV also exist between different measuring techniques. The PV measured by the schlieren imaging technique (3.2-14 m/s for males and 2.2-5 m/s for females) (Tang et al. 2012) was much smaller than those measured by PIV (Han et al. 2021)(Khan et al. 2004)(Zhu et al. 2006)(Chao et al. 2009)(Vansciver et al. 2011)(Kwon et al. 2012)(Wang et al. 2020). The authors claimed that subjects coughing in PIV measurement were somehow constrained and unnatural due to the measurement setup, while the cough flow was obtained more naturally in Schlieren imaging study. However, the relative temperature difference between the exhaled cough air and surrounding ambient air might influence the visualization of the cough flow, and consequently, influence the accuracy of peak velocity measurement by the Schlieren imaging technique. Therefore, the uncertainties of measuring techniques require further investigation.

The flow rate or velocity rapidly reaches a peak value early in the cough, therefore, the peak velocity time PVT is very small compared with the total cough duration time CDT. The PVT was reported by Mahajan et al. (1994), Gupta et al. (2009b) and Han et al. (2021). Large deviation exists between different studies. Gupta reported a larger PVT (57-110 ms), which is more than double the values of the other two studies. Similar to PVT, CDT also presents a large variation among different studies. The CDT value ranged from 200 ms to 900 ms, where the average value was around 500-550 m. The lowest CDT was measured by Tang et al. (2012) with the schlieren imaging technique. The authors pointed out that the limitation of such a technique is that the visibility of shadowgraphs disappeared when the exhaled and surrounding air temperatures equalized. Therefore, it is difficult to capture the entire cough process by Schlieren imaging. On the other hand, even though the peak cough flow for females was weaker than that for males, PVT or CDT didn't present clear gender difference, indicating that their cough duration times were almost the same.

2.2 Cough flow direction

Gupta et al. (2009b) measured the cough flow direction by smoke visualization. The cough flow presented as a downward jet and was defined by the angles between upper and lower boundaries to the horizontal lines, as shown in Figure 2 (a). The values of θ1 and θ2 were around 15 ° and 40 °, respectively. (The vertical cough spread angle θ_V was around 25 °). Different from cough flow rate, little variation in the cough spread angels were observed in this study. The jet had negligible spread in the width, where the horizontal cough spread angle was around 0 ° (θ=90 °).

Velocity vectors measured by PIV was used to analyze the flow direction. Kwon et al. (2012) described the cough flow by the angles of upward vector and downward vector, as shown in Figure 2 (b). The cough flow presented as a jet almost symmetrical in the y-direction, where

the vertical cough spread angle was around 38º for males and 32º for the females. Han et al. (2021) introduced a more quantitative method to determine the cough boundaries, where the flow boundary was defined as the position where the velocity decayed to 1 % of the maximum value at the flow centerline, as shown in Figure 2 (c). The influence of the head position variations was eliminated by utilizing the fitting line method. The cough flow direction was described by vertical cough spread angles θ_V and horizontal cough spread angles θ_H. Different from Gupta's results, individual differences were significant in this study. The average vertical/horizontal cough spread angle was 15.3◦/13.3◦ for males and 15.6◦/14.2◦ for females. The angles were smaller than the ones measured in the other two studies.
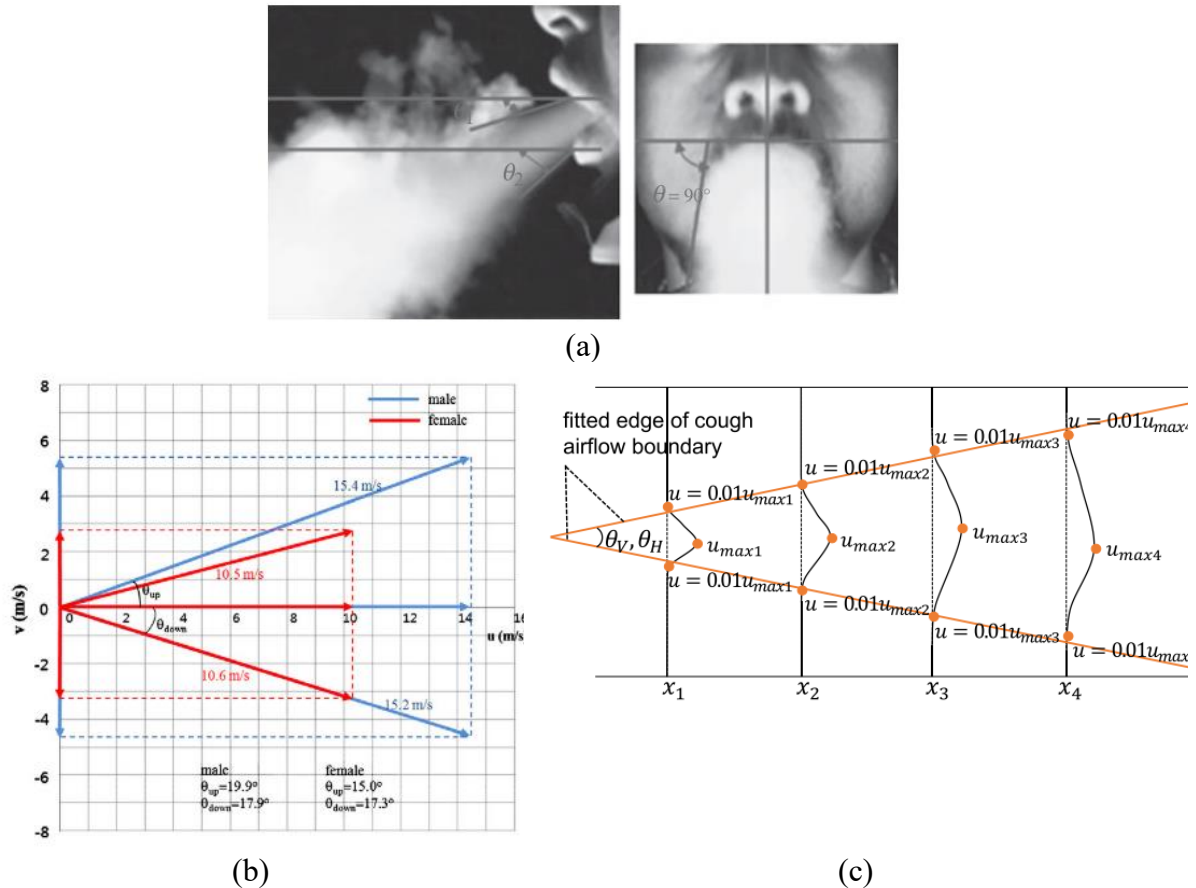

(a)

(b)

(c)

Figure 2. Schematic of determination of cough flow direction in the literature (a) Gupta et al. (2009b) (b) Kwon et al. (2012) (c) Han et al. (2021)

2.3 Mouth opening

Mouth geometry affects the cough flow dynamic, such as cross-sectional profile, hydraulic diameter, direction, and turbulence levels. Consequently, it affects aerosol distribution and penetration.

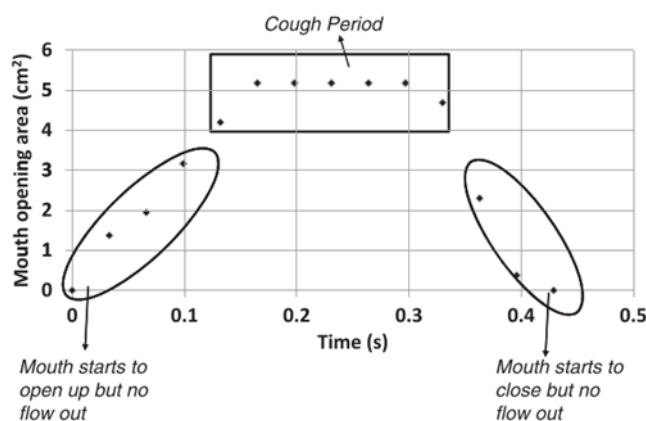The mouth ope~~ning area during a cough was measured by Gupta et al. (2009~~a), as shown in

Figure 3. Even mouth opening changed during a cough, the opening area was almost constant when there was flow from the mouth. There is a variation in mouth opening area during a cough with the gender. The mean opening area for female subjects was smaller than that of male subjects, which was 3.37 cm2 for females and 4 cm2 for male.
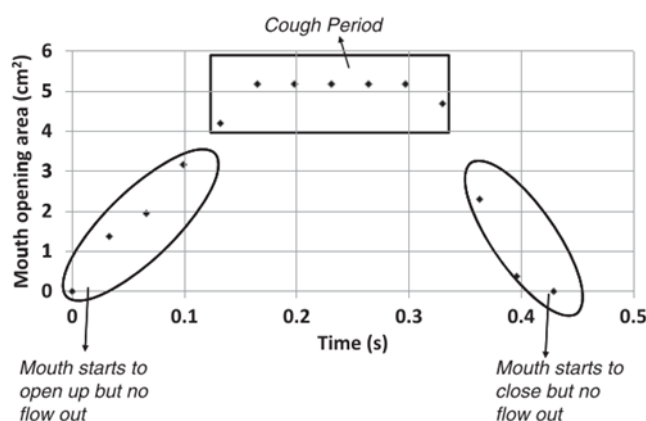

Figure 3. Month opening area during a cough (Gupta et al. 2009a)

Instead of the opening area, the mouth width was measured in Han's study (2021) and used as the boundary condition in CFD simulation. However, the measurement was done without coughing, but just as the characteristics of human subjects. In addition, the mouth width could not provide sufficient information on mouth geometry during a cough since the distance between lips also matters significantly.

It is clear to see that there are large deviations on mouth geometry between subjects and no agreement on how to report the mouth geometry during a cough. On the other hand, most studies only focus on the geometry created by lips, since it is the boundary of the mouth outlet. However, the flow travels through the trachea and oral cavity (including teeth, tongue, and lips), and the flow structure and dynamic are certainly influenced by them. Wei and Li (2017) pointed out that the difference in the spread angle of the model and human subject may be due to the missing complex oral cavity, including the effect of teeth.

2.4 Vortex structure

Several studies (Prasanna Simha and Mohan Rao 2020)(Khan et al. 2004)(Thacher and Mäkiharju 2022)(Tan et al. 2021) mentioned that the circulating motion of vortex rings produced by coughs can enhance the transport of cough droplets. Vortex rings are typically produced by injecting fluid into a quiescent medium for a short duration. The vortex rings generated by cough is due to the vibrations in the airway passage leading to periodic constrictions and relaxations, which create flow variations.

In Padmanabha's study (2020), a periodic vortex ring ejection phenomenon was observed by the schlieren imaging technique that appears as a pulsation of the cough airflow. These pulsations start several milli-seconds after the initiation of the cough. The periodic ejection and motion of vortex rings can be seen in Figure 4. The velocity of propagation of viscous vortex rings can be expressed by an analytical approach, which a function of time (t), initial radius (R), vortex ring circulation (χ), and kinematic viscosity (v).
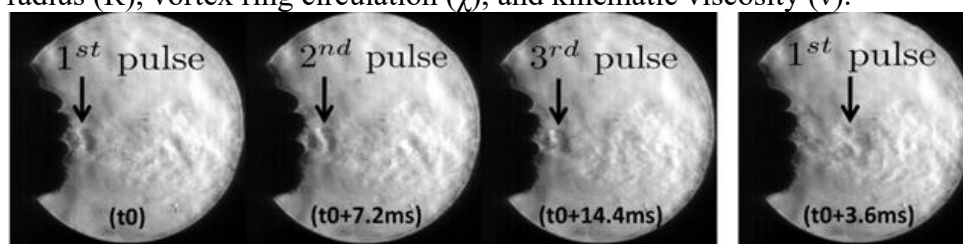

Figure 4. Periodic ejection and motion of vortex rings in coughs by Schlieren image video (Prasanna Simha and Mohan Rao 2020)

An important parameter in the dynamics of vortices is vorticity, a vector that describes the local rotary motion at a point in the fluid. The instantaneous vorticity was plotted in Figure 5 by Khan et al. (2004). It can be seen that maximum vorticity corresponds to the peak flow rate/velocity and occurs in the region of the shear layer, and the center region of cough flow is nearly void of vorticity.
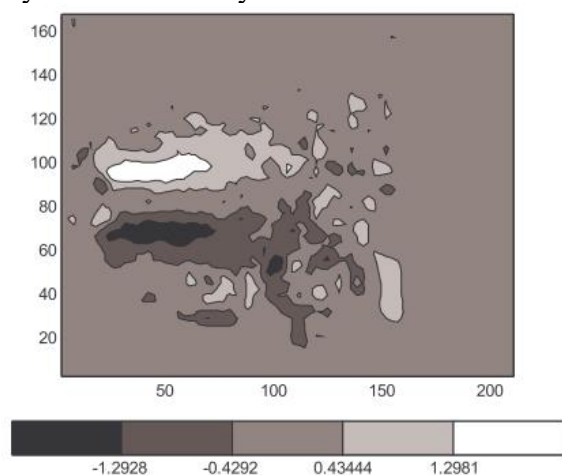

Figure 5. Vorticity contour plot displaying initial vortices (unit 1/s) (Khan et al. 2004)

Cough is often described as impulsively started jets. Tan et al. (2021) compared dispersion of aerosol particles from a loud cough with classical vortex ring formation on starting jet, as shown in Figure 6. The black particles represent virtual aerosol droplets, while the background scalar shows the out-of-plane vorticity field. From the classical vortex ring formation from impulsively started jet (Figure 6 lower), it could see that the flow structure depends on the stroke ratio L/D where is the ratio between the length of ejected fluid and the ejection diameter. When L/D is less than 4 , the jet presents as a short puff and all momentum are absorbed into the vortex ring. When L/D approximately equal to 4 , the maximum amount of momentum has been absorbed and the vortex ring begins to trail a thin tail. When L/D is larger than 4 , the vortex ring is unstable and sheds off smaller vortices. The L/D for a loud cough is estimated with a magnitude of 160, therefore, a loud cough contains much higher momentum than a single vortex ring could entrain.
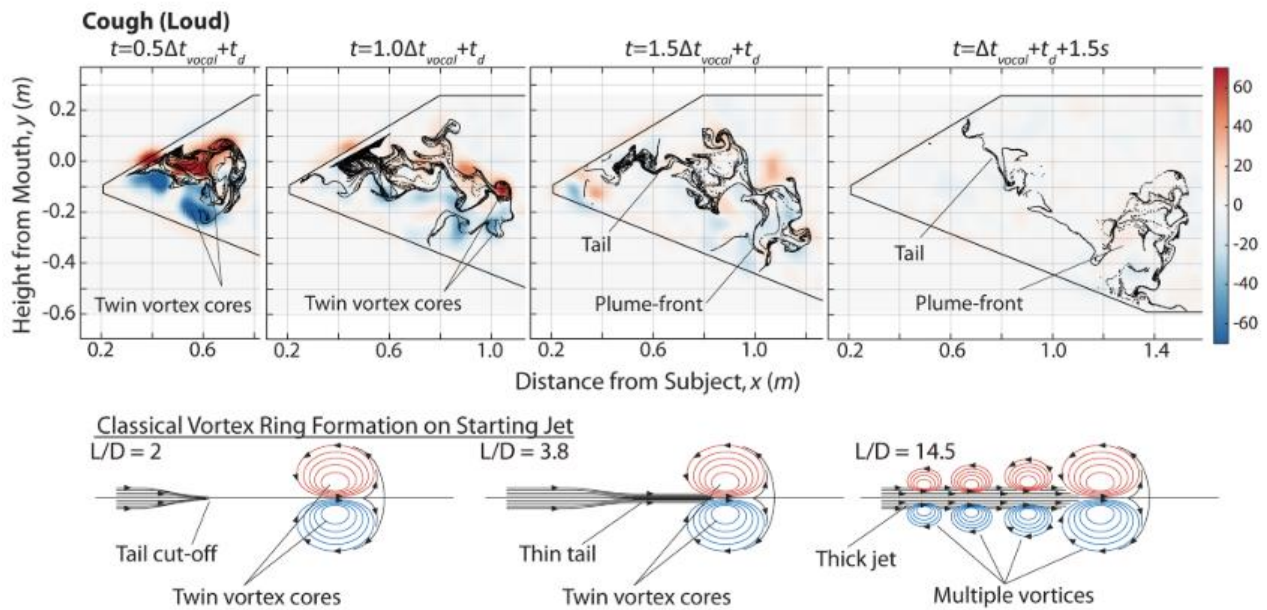
Figure 6. Dispersion dynamics of aerosol particles for a loud cough compared with classical vortex ring formation on starting jet (Δt_{vocal} is the total duration of the subject's cough, t_d is the instance that the plume enters the measurement domain, stroke ratio L/D where L is the length of ejected fluid and D is ejection diameter) (Tan et al. 2021)

Figure 6 shows, when $t=+0.5\Delta t_{vocal}$, the cough flow first presents a dominant vortex ring similar in structure to the classical impulsively start jet. The vortex ring quickly disintegrated into multiple smaller vortex cores starting at +1.0 Δt_{vocal}. At +1.5 Δt_{vocal}, the original vortex ring structure has become indistinguishable. However, the aerosol particles continued to move forward even at +1.5s after cough, and the presence of a trail is an indication of high L/D impulsively started jets. Their results indicate that virus-laden aerosol ejected during coughs remain concentrated within the moving plume-front. A high exposure risk is expected with direct collision in the moving plume-front.

3   CONCLUSIONS

The literature review leads to the following conclusions:
- The airflow characteristic of human cough is normally measured by three techniques, including the Schlieren imaging technique, spirometer and PIV. Each technique has its advantages and disadvantages, and the uncertainties of measuring techniques require further investigation. On the other hand, PVT and CDT are in the order of milliseconds. In order to capture the cough characteristic, it is essential to have high-frequency measurements.
- The cough profile can be described by a gamma-probability distribution function. The characteristic of the profile can be defined by the following parameters: peak flow rate (PFR) or peak velocity (PV); peak velocity time (PVT), and cough duration time (CDT) and cough expired volume (CEV). Large deviations have been shown on PFR, PV, CEV due to subjects' gender, height, age and body mass surface, however, some deviations are due to different measuring techniques.
- Large deviations on flow direction and mouth geometry between different studies and no agreement on how to report these parameters during a cough.

- Cough creates vortex rings due to the vibrations in the airway passage leading to periodic constrictions and relaxations. The circulating motion of vortex rings can enhance the transport of cough particles in the indoor environment.

4 ACKNOWLEDGEMENTS

5 REFERENCES

Bianchi, Carlo, and Paola Baiardi. 2008. "Cough Peak Flows: Standard Values for Children and Adolescents." *American Journal of Physical Medicine and Rehabilitation* 87(6):461–67. doi: 10.1097/PHM.0b013e318174e4c7.

Centers for Disease Control and Prevention (CDC). 2021. "Scientific Brief : SARS-CoV-2 Transmission." Retrieved (https://www.cdc.gov/coronavirus/2019-ncov/science/science-briefs/sars-cov-2-transmission.html#anchor_1619805200745).

Chao, C. Y. H., M. P. Wan, L. Morawska, G. R. Johnson, Z. D. Ristovski, M. Hargreaves, K. Mengersen, S. Corbett, Y. Li, X. Xie, and D. Katoshevski. 2009. "Characterization of Expiration Air Jets and Droplet Size Distributions Immediately at the Mouth Opening." *Journal of Aerosol Science* 40(2):122–33. doi: 10.1016/j.jaerosci.2008.10.003.

Gupta, J. K., C. H. Lin, and Q. Chen. 2009a. "Flow Dynamics and Characterization of a Cough." *Indoor Air* 19(6):517–25. doi: 10.1111/j.1600-0668.2009.00619.x.

Gupta, J. K., C. H. Lin, and Q. Chen. 2009b. "Flow Dynamics and Characterization of a Cough." *Indoor Air* 19(6):517–25. doi: 10.1111/j.1600-0668.2009.00619.x.

Han, Mengtao, Ryozo Ooka, Hideki Kikumoto, Wonseok Oh, Yunchen Bu, and Shuyuan Hu. 2021. "Measurements of Exhaled Airflow Velocity through Human Coughs Using Particle Image Velocimetry." *Building and Environment* 202(May):108020. doi: 10.1016/j.buildenv.2021.108020.

Khan, T. A., H. Higuchi, D. R. Marr, and M.N.Glauser. 2004. "Unsteady Flow Measurement of Human Micro Environment Using Time Resolved Particle Image Velocimetry." Pp. 88–100 in *Roomvent 2004*. Vol. 4.

Kwon, Soon Bark, Jaehyung Park, Jaeyoun Jang, Youngmin Cho, Duck Shin Park, Changsoo Kim, Gwi Nam Bae, and Am Jang. 2012. "Study on the Initial Velocity Distribution of Exhaled Air from Coughing and Speaking." *Chemosphere* 87(11):1260–64. doi: 10.1016/j.chemosphere.2012.01.032.

Lindsley, William G., Francoise M. Blachere, Robert E. Thewlis, Abhishek Vishnu, Kristina A. Davis, Gang Cao, Jan E. Palmer, Karen E. Clark, Melanie A. Fisher, Rashida Khakoo, and Donald H. Beezhold. 2010. "Measurements of Airborne Influenza Virus in Aerosol Particles from Human Coughs." *PLoS ONE* 5(11). doi: 10.1371/journal.pone.0015100.

Mahajan, R. P., P. Singh, G. E. Murty, and A. R. Aitkenhead. 1994. "Relationship between Expired Lung Volume, Peak Flow Rate and Peak Velocity Time during a Voluntary Cough Manoeuvre." *British Journal of Anaesthesia* 72(3):298–301. doi: 10.1093/bja/72.3.298.

Muthusamy, Jayaveera, Syed Haq, Saad Akhtar, Mahmoud A. Alzoubi, Tariq Shamim, and Jorge Alvarado. 2021. "Implication of Coughing Dynamics on Safe Social Distancing in an Indoor Environment—A Numerical Perspective." *Building and Environment* 206(April):108280. doi: 10.1016/j.buildenv.2021.108280.

Oh, Wonseok, Ryozo Ooka, Hideki Kikumoto, and Mengtao Han. 2022. "Numerical

Modeling of Cough Airflow: Establishment of Spatial–Temporal Experimental Dataset and CFD Simulation Method." *Building and Environment* 207(PB):108531. doi: 10.1016/j.buildenv.2021.108531.

Prasanna Simha, Padmanabha, and Prasanna Simha Mohan Rao. 2020. "Universal Trends in Human Cough Airflows at Large Distances." *Physics of Fluids* 32(8). doi: 10.1063/5.0021666.

Tan, Zu Puayen, Lokesh Silwal, Surya P. Bhatt, and Vrishank Raghav. 2021. "Experimental Characterization of Speech Aerosol Dispersion Dynamics." *Scientific Reports* 11(1):1–12. doi: 10.1038/s41598-021-83298-7.

Tang, Julian W., Andre Nicolle, Jovan Pantelic, Gerald C. Koh, Liang de Wang, Muhammad Amin, Christian A. Klettner, David K. W. Cheong, Chandra Sekhar, and Kwok Wai Tham. 2012. "Airflow Dynamics of Coughing in Healthy Human Volunteers by Shadowgraph Imaging: An Aid to Aerosol Infection Control." *PLoS ONE* 7(4). doi: 10.1371/journal.pone.0034818.

Thacher, Eric, and Simo A. Mäkiharju. 2022. "Effect of Coherent Structures on Particle Transport and Deposition from a Cough." *Aerosol Science and Technology* 56(5):425–33. doi: 10.1080/02786826.2022.2044449.

Vansciver, Meg, Shelly Miller, and Jean Hertzberg. 2011. "Particle Image Velocimetry of Human Cough." *Aerosol Science and Technology* 45(3):415–22. doi: 10.1080/02786826.2010.542785.

Wang, Hongping, Zhaobin Li, Xinlei Zhang, Lixing Zhu, Yi Liu, and Shizhao Wang. 2020. "The Motion of Respiratory Droplets Produced by Coughing." *Physics of Fluids* 32(12). doi: 10.1063/5.0033849.

Wei, Jianjian, and Yuguo Li. 2017. "Human Cough as a Two-Stage Jet and Its Role in Particle Transport." *PLoS ONE* 12(1). doi: 10.1371/journal.pone.0169235.

WHO. 2021. "Coronavirus Disease (COVID-19): How Is It Transmitted?" Retrieved November 2, 2022 (https://www.who.int/emergencies/diseases/novel-coronavirus-2019/question-and-answers-hub/q-a-detail/coronavirus-disease-covid-19-how-is-it-transmitted).

Zhu, Shengwei. 2006. "Investigation into Airborne Transport Characteristics of Airflow Due to Coughing in A." *Measurement* 112.

Zhu, Shengwei, Shinsuke Kato, and Jeong-Hoon Yang. 2006. "Investigation into Airborne Transport Characteristics of Airflow Due to Coughing in a Stagnant Indoor Environment." 112.